Shahrood University of Technology

Iranian Society of Mining Engineering (IRSME)

THOMSON REUTERS

A Numerical Investigation of TBM Disc Cutter Life Prediction in Hard Rocks

Masood Zahiri Galeshi[1], Kamran Goshtasbi[2*], Jafar Khademi Hamidi[2] and Kaveh Ahangari[1]

1- Department of Mining Engineering, Science and Research Branch, Islamic Azad University, Tehran, Iran
2- Department of Mining Engineering, Faculty of Engineering, Tarbiat Modares University, Tehran, Iran

Article Info	Abstract

There is a direct relationship between the efficiency of mechanized excavation in hard rocks and that of disc cutters. Disc cutter wear is an important effective factor involved in the functionality of tunnel boring machines. Replacement of disc cutters is a time-consuming and costly activity that can significantly reduce the TBM utilization and advance rate, and has a major effect on the total time and cost of the tunneling projects. When these machines bore through hard rocks, the cutter wear considerably affects the excavation process. To evaluate the performance of the cutters, first, it is essential to figure out how they operate the rock cutting mechanism; secondly, it is important to identify the key factors that cause the wear. In this work, we attempt to introduce a comprehensive numerical method for estimation of disc cutter wear. The field data including the actual cutter wear more than 1000 pieces and the geological parameters along the Kani-Sib transmission tunnel in the northwest of Iran are compiled in a special database that is subjected to a statistical analysis in order to reveal the genuine wear rule. The results obtained from the numerical method indicate that with an increase in the wear of disk cutter up to 25 mm, the applied normal and rolling forces can be multiplied by 2.9 and 2.7, respectively, and by passing the critical wear, the disk cutters lose their optimal performance. This method also shows that confining pressure will increase the wear of the disc cutter. By the proposed formulation, the cutter consumption rate can be predicted with a high accuracy.

1. Introduction

The increase in the mountain roads and underground transportation, and water transport tunnels, and the need to create new routes and long tunnels have led to the development of tunnel boring machines (TBMs) since the early 19th century [1]. A TBM machine is one of the most common equipment in the tunneling industry, which is used in various dimensions of tunnel and ground conditions from soft soils to hard rocks [2]. Despite the high initial investment, due to its high rate of advance, high productivity factor, permanent maintenance system installation during excavation, final tunnel shape, and low impact on the environment and safety, this method is competitive with the conventional tunneling methods.

As an operator, the most important challenge in using these machines is to select an appropriate machine according to the ground conditions and to predict its performance parameters. However, as a manufacturer, the main challenge of designing the machine (head diameter, number of discs, thrust, torque, and disk spacing) is the most important part of the job. Understanding the interaction between the rock and disk is what can respond to the designer's and user's concerns. During excavation with TBMs, disc cutters roll over the rock surface in order to create a crushed zone. Cracks start with the crushed zone and extend through downwards and sides. By connecting the cracks, the rock chips are separated and discharged [1]. Successful applications of TBMs have been reported in the tunnels less than 1 m up to

✉ Corresponding author: goshtasb@modares.ac.ir (K. Goshtasbi).

14 m in diameter [3-6]. However, in some projects, TBMs have encountered hard rocks with a uniaxial strength up to 400 MPa, resulting in higher unacceptable disk wear rates. If the disc cutter abrasion exceeds a certain level, it will no longer work for rock cutting. In the disk cutter replacement time, in addition to the cost of repair or replacement, the contractor must also endure the cost of device downtime [5]. Statistically, the cost of damaged cutters is at least one-fifth of the cost of the project [7]. However, in some projects in granite such as the Qinling Tunnel in China, this cost has been reported to be one-third [8]. On the other hand, the time taken to replace the cutters is approximately one-third of the total project time [7]. As a result, the impact of the cutter wear conditions on the rock failure is an important issue for the TBM efficiency to improve. However, due to the sensitivity of the data that the TBM manufacturers are dealing with and the difficulty of measuring the actual wear during TBM excavation, the researchers have a limited access to the cutter wear data [9]. The cutter wear not only directly affects the project, for example through cutter costs and personnel costs associated with replacing the worn cutter, but can also affect the work cycle and performance of the rock excavation [10]. Therefore, an accurate estimation of the cutter life under different conditions is extremely important. There are many empirical models to estimate wear. The most common cutter wear models are CSM [2], NTNU [1], and Gehring [11].

Hassanpour et al. [12] have summarized the common cutter wear estimation models and have extended an experimental TBM cutter wear estimation model for the pyroclastic and mafic igneous rocks. Despite the studies, it is certain that the accuracy of different cutter wear estimation models is not currently satisfactory [13] since most of these models are based on the correlations with a coefficient of wear such as the Cerchar abrasion index, and the effects of other important parameters involved have been Ignored [9, 12]. However, the disc cutter wear is affected by two groups of factors including the geological conditions (including the intact rock parameters, rock mass parameters, and environmental factors) and the TBM performance parameters (including RPM, thrust, and penetration depth) [14].

Despite the fact that the experimental, laboratory, and analytical models have played a significant role in understanding the disc and rock interaction, due to the deficiencies such as the cost and efficiency in certain situations, the researchers are looking for more comprehensive and cost-effective methods. In the recent years, the development of the hardware and software capabilities and the development of the numerical methods have identified them as a viable alternative. The numerical models capable of accurately simulating the rock crushing process facilitate the evaluation of the TBM performance [15]. Various methods such as the finite difference method (FDM), displacement discontinuity method (DDM), discrete element method (DEM), and finite element method (FEM) have been used to simulate the shear process. For example, Park et al. [16] have extended a heterogeneous 2D model using FLAC in order to investigate the effect of limiting pressure and disc cutter spacing on the rock crushing. Gang et al. [17-19] have investigated the effect of joint spacing and its orientation on the crack initiation and expansion as well as the crushing pattern using 2D UDEC. Eftekhari et al. [20] have investigated the impact of randomly joint propagation on rock mass on the rock shear pattern using UDEC. Li et al. [21] have used DEM in order to simulate the TBM advance process and have concluded that the tensile cracks arise from the chip process and shear cracks from the crushing force. Su and Akcin [22] and Mendoza [23] have used a 3D DEM (PFC3D) code in order to predict the cutter forces in the shear test. Chao et al. [24] have employed a software with an explicit time integration FEM (AUTODYN-3D) in order to simulate the rock fracture process observed during the LCM test. Menzes et al. [25] and Jamie et al. [26] have modeled the initiation and expansion of cracks and dynamic crushing in excavation using the explicit LS-DYNA finite element code. Yu [27] has applied the LS-DYNA software in order to model the overall rotation of the cutter head during rock cutting.

Despite many studies, few studies have been conducted on the cutter consumption rate. Table (1) presents the studies performed in this area from the old to the new with their weaknesses. According to the research works, modeling the disc cutter wear phenomenon requires further investigations. Given the weaknesses of the previous methods in the accurate estimation of the cutter life in hard rocks and various conditions of the boring machine, in this work, we attempted to model the rate of disk cutter consumption numerically according to the actual conditions of the problems such as confining pressures, non-linear rock behavior, and disk conditions. Therefore, the contact mechanics and tool wear were implemented in the FEM framework. For this purpose, after the introduction section, the disk-rock contact theory is explained, and a comprehensive formula for the calculation of disk cutter wear is presented. The introduced parameters include three different groups of mechanical and geometrical ones, numerical parameters, and operational parameters. The mechanical and geometrical parameters were obtained from the laboratory measurements. The second group parameters also require the numerical modeling to

reproduce. Since the rock-cutting process is a complex dynamic process with non-linear properties, the numerical modeling of this problem must be capable of computing this complex behavior under varied conditions. Therefore, the explicit dynamic finite element method (LS-DYNA) was used for modeling. The operational parameters are also required to be calibrated with the real data. For this purpose, during the construction of the Kani-sib Tunnel project in northwestern Iran, a special database containing an actual cutter wear and geological data was collected and analyzed from different layers of the tunnel. In Section 3, in order to illustrate the validity of the proposed model, the results obtained were compared with the previously existing methods and the actual tunneling data. Finally, Section 4 discusses the wear rate of disk cutters in different situations and discusses the effective conditions. Section 5 concludes this paper.

2. Governing equations on wear phenomenon

From the perspective of contact mechanics, when two objects are in contact with each other, two types of slip and roll motion can occur. The relative motion of two objects that are in contact with each other is called rolling, which is along the parallel axis of the tangent plane, while the sliding displacement is the point of contact between the two planes [37]. It is clear that rolling and sliding occur simultaneously between the rock and cutter contact. The slip ratio for rolling objects is equal to the slip area to the total rolling distance [15, 38, 39]. Therefore, the slip velocity S can be calculated by the contact theory as follows [37, 39]:

$$S = \xi V \tag{1}$$

where V is the tangent speed of the disc cutter and ξ is the slip ratio; they can be calculated as follow:

$$\xi = \frac{\mu a}{R}\left[1 - \left(1 - \frac{F_r}{\mu F_n}\right)^{1/2}\right] \tag{2}$$

$$V = 2\pi R' N \tag{3}$$

where μ is the friction coefficient, a is the width of the contact area, F_r is the rolling force applied to the

disc, F_n is the normal force applied to the disc, R' is the distance between the center of the cutter head to the location of the disc, i.e. the disc cutter installation radius, and N is the TBM rotation per minute. R is also the radius of the disc cutter including the wear, and some researchers have indicated R-H, in which H is the value of the cutter disc wear at the calculation time. According to Figure 1, the value of "a" can be calculated as follows:

$$a = \theta R, \quad \theta = \cos^{-1}(\frac{R - P}{R}) \tag{4}$$

where θ is the central angle between the rock and the disc contact, and P is the penetration depth.

Assuming a related relationship between the wear volume of the disc cutter and the frictional force that is related to the material properties, the wear rate energy is introduced as the related relationship between the size of the disc cutter's abrasive volume and the frictional force [39]. The volumetric wear of the disc cutter M during the tunneling process can be expressed as follows:

$$M = K I W \tag{5}$$

where I is the wear energy, which is defined as the volume of wear of the disc cutter per unit of the frictional power under the laboratory conditions. K is a factor that depends on the material stiffness that is 1 if the cutter ring is completely homogenous. W is also the frictional force. According to the friction law, the frictional slip force is created by the friction force and the slip distance. Thus the frictional force can be expressed as follows:

$$W = \mu F_n S t \tag{6}$$

where t is the drilling time, which can be calculated as follows [15, 29, 34, 39]:

$$t = L/V_0, \quad V_0 = p_{rev}.N, \quad p_{rev} = Pm \tag{7}$$

where L is the excavated tunneling length, V_0 is the cutter head speed, p_{rev} is the penetration depth per rotation, and m is the number of disc cutters used in the cutter head. It is noteworthy that μ and I can be measured for a given rock and material.

Table 1. Common models for disc cutter wear estimation.

| Ref.	Required geo-mechanical testing	Input geo-mechanical parameters	Cutter wear output parameters	Restrictions
[28]	Petrographic analysis and point load testing	Quartz content, grain dimensions, and point load index	Wear rate	It is not valid right now because it is based on the old assumption of wedge theory for the cutting process
[29]	Cerchar abrasion test, uniaxial compressive strength (UCS), and point load test	Cerchar abrasion index (CAI), UCS, tensile strength (σ_{PLT})	Rolling distance	---
[30]	-	-	Overall cost, delays, and total number of cutter replacements	An experimental method for estimating cutter life that is not publicly available
[11]	Cerchar abrasion test, and UCS	UCS, CAI	Average life of ring cutter	Dependence of the coefficient on the limiting pressures and the assumption of uniform sex discs at the cross-section
[2]	Cerchar abrasion test	CAI	Average rolling distance, total cost, delays, and total number of cutter replacements	Cutter lifetime dependence on single parameter (CAI)
[1]	Sievers' J (SJ) small scale excavation test and AVS test	Cutter life index (CLI)	Average cutter ring life, total cost, delays, and total number of cutter replacements	It is mainly based on Norwegian igneous and metamorphic rocks data, and requires relatively sophisticated NTNU tests and methods.
[31]	Sievers' J point test	SJIP starting point, steepest SJIP gradient	Cutter life index	Complexity of tests required
[32]	Cerchar abrasion test and UCS test	CAI, UCS	Average rolling distance	
[33]	Cerchar abrasion test, UCS, brittle test (S_{20}), and small scale SJ test	CAI, UCS, DRI	Cutter use	Restrict data to a specific project
[14]	Cerchar abrasion test	CAI	Cutter net life, total number of cutter replacements, and total cost	Dependence of output values only on CAI
[34]	-	Specific total energy of cutter head (E_s)	Average wear rate and number of disabled cutters	Unrealistic cutter wear estimation
[12]	Vickers hardness test and UCS test	Vickers hardness number (VHNR), UCS, ABI	Average cutter ring life	Project-related data
[35]	UCS test	UCS	Wear rate	An experimental method with a low correlation coefficient between the output parameter and the only input parameter
[15]	Cutter disc forces	TBM parameters and abrasion energy	Average rolling distance	Analytical solution of the wear process and the existence of simplifying assumptions
[36]	Brittleness test (S_{20}), UCS, abrasion index, SJ, and AVS test	Cutter life index (CLI)	Average cutter ring life, total cost, delays, and total number of cutter replacements	Complexity of tests and proposed methods
[13]	Cerchar abrasion index, UCS	CAI, UCS	Cutting consumption rate (E_f)	Data constraints related to a granite rock tunneling project in China
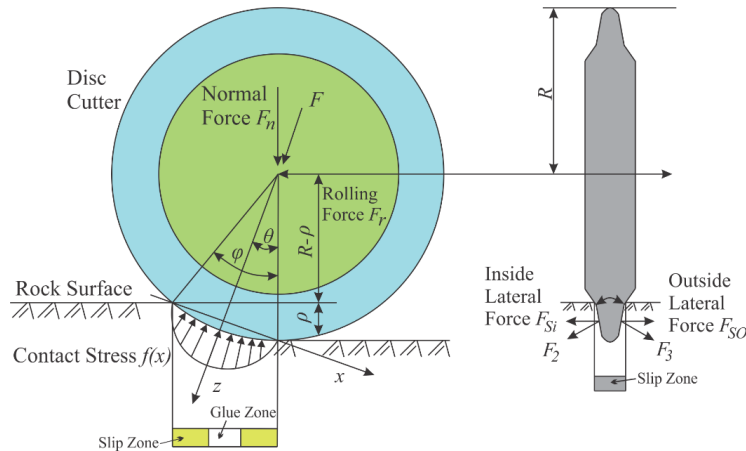
Figure 1. A general view of the contact area between a single disc cutter and rock.

Finally, using the above equations and expanding Equation (5), we will finally have:

$$M = \frac{2\pi \, K \, I \, \mu^2 \, F_n \, R' \, L . \cos^{-1}\left(\frac{R-P}{R}\right) . \left[1 - \sqrt{1 - \frac{F_r}{\mu \, F_n}}\right]}{(P.m)} \quad (8)$$

According to the estimated formula of Roxborough and Phillips [40], the ratio of the rolling force F_r to the normal force F_n will be as follows:

$$\frac{F_r}{F_n} = \sqrt{\frac{P}{2R - P}} \quad (9)$$

This relation can be used to simplify the relationship (8) but this simplification is ignored since the values for the F_n and F_r forces can be obtained with a high accuracy from the numerical modelling. In addition, Equation (9) was developed for the V-shaped disc cutters, and its use for the CCS-type discs would result in unrealistic results.

3. Numerical modeling

The three factors affecting the excavation process include the geological properties, features of the boring machine, and executive factors. These factors are shown in Figure 2. In order to calculate the disc cutter wear in a specific condition using Equation (8), the most important factors to be calculated are the forces applied to the disc cutter by rock and wear coefficient (K). As mentioned above, the explicit dynamic finite element method (LS-DYNA) is used to accurately calculate the forces on the disk. A high flexibility in simulation, ability to calculate the non-linear behavior of materials, applying different boundary conditions and dynamic conditions, adaptation of Lagrangian,

and Eulerian formulations were the reasons for choosing this method.

3.1. Geometry and meshing

In the case of the rock-disc interaction problem, in which the rock spalling mechanism is also part of the problem, determination of the mesh size plays an important role. Obtaining acceptable results is related to two basic characteristics of the mesh: size and type of element. One of the most important steps in the simulation of rock cutting is the use of element erosion to show the crushing mechanism. Thus the level of rock erosion and the likely path of failure should be as real (and not identical) as possible. In order to achieve this goal, the smallest non-cubic element would be ideal. Such a conclusion can be seen in the previous research works [26, 41-44]. Many researchers believe that the orthogonal shape of solid hexagonal elements with constant stress (software defaults) makes it impossible to reproduce the rock particle heterogeneity [45]; so the tetrahedral elements with one integration point were chosen. However, avoiding the high number of elements for reducing the run time will be critical. Many researchers believe that in addition to the accuracy and convergence of the solutions, the size of the elements is limited to the actual size of the rock particles in the analysis involving the erosion of the element [26, 41, 46]. Cho *et al*. in the shear modeling of granite have stated that the elements with a unit volume of 0.027 m^3 are small enough to guarantee the accuracy of the numerical simulations [47]. Therefore, the rock sample was meshed with 195575 tetrahedral elements (37503 nodes) to thereby guarantee the volume limit for each element.
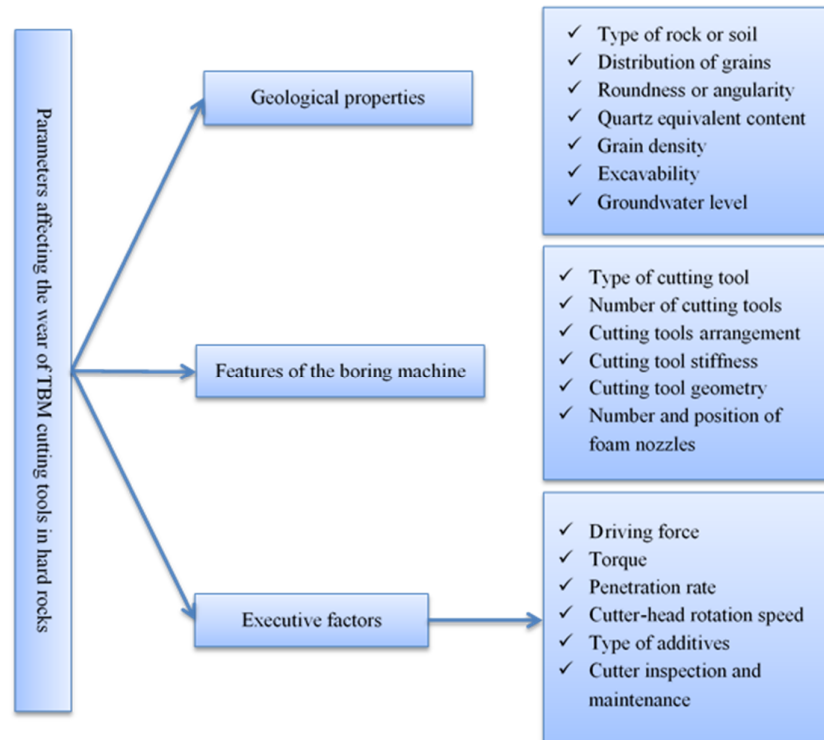
Figure 2. Different effective parameters in a mechanized excavation process.

Richard et al. [48] have stated that in modeling the shear phenomenon, the shear force must be divided by a distance that is at least greater than the shear depth (P). Therefore, the minimum horizontal dimension l of the numerical model is consistent with the l/P≥10 ratio. The dimensions of the rock sample were selected according to this criterion. In addition, since in the first step, the aim is to validate the proposed method, in order to compare the results of the constructed model, it should be in accordance with the previous research works [2, 24, 47]. It is important to emphasize that regardless of the different cutting parameters such as the depth of penetration and the geometry of the cutter (change due to erosion), the elements must be approximately constant in size. This fact significantly affects the fracture mode both in the brittle and ductile states. In other words, in order to compare the results of the numerical modelling at different penetration depths and different abrasions of the disc cutter, the size of the elements must have the same dimensional characteristics. The dimensions and mesh size are presented in Figure 3. It should be noted that the dimensions of the disc cutter are modeled in accordance with reality (17 inches in diameter). However, in the next step, for the wear rate calculation, the numerical model is considered as in Figure 4 to make it closer to reality.

3.2. Boundary conditions and modeling details

The boundary conditions of the rock sample and the disk cutter are presented in Table (2). In addition, the floor and sidewall surfaces in the rock sample was defined as non-reflection boundaries, allowing stress waves to damp rather than reflect. This boundary does not affect the stress distribution near the corners of the model. Finally, before analysis, the gravitational force (g = 9.81 m/s^2) was applied to the rock slab through the early stages.

After creating the geometry, performing the meshing according to the criteria and applying the boundary conditions of the modeling, the following steps were taken: defining the constitutive models and material behavior and applying them to the model; defining the contact type or algorithm; specifying the type of elements and integration. Based on the laboratory tests and the available information, the kinematic plastic material model was chosen for this problem. This behavioral model permits the elastic and plastic deformations of the material. In addition, the model is able to simulate the erosion of the elements and the damage mechanism by calculating the strain in

failure. In addition, this method has a considerable ability in simulating the contact of the components of the model. Since the proposed method was required to be validated, in the first step, the applied forces on a rigid disk cutter were calculated numerically in the cutting process of a hard rock specimen. The results obtained from the proposed method were compared with those for the laboratory tests and the previous methods. After ensuring the accuracy of the results of the applied

forces on the cutter, the actual mechanical properties of the rock specimen and the disk cutter were entered into the model to simulate the cutter consumption rate. At this stage, with the progress of wearing, the geometry of the cutter was updated. In order to compare the results of the wear rate in hard rock, the real data was used, which was related to the Kani-Sib water transfer tunnel project in the northwestern Iran.
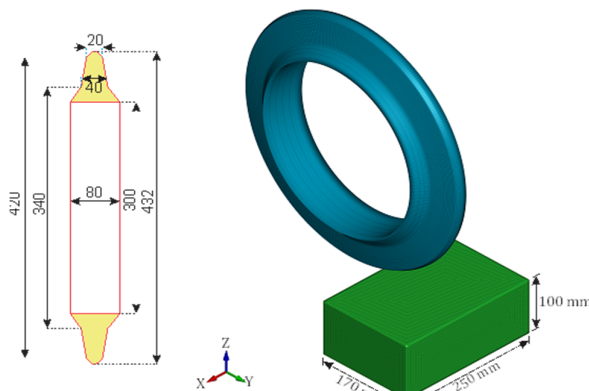
Figure 3. Geometry and mesh of a rock sample with a real-size disc cutter (dimensions in mm).
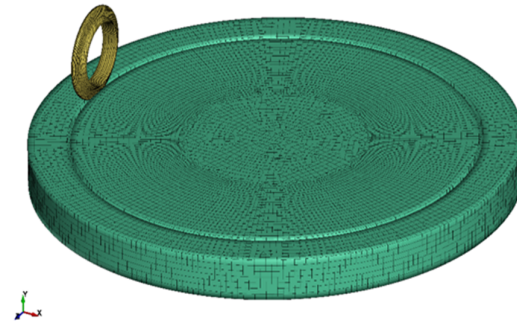

Figure 4. Numerical model used for wear rate calculation.

Table 2. Node degrees of freedom in the finite element model.

Degree of freedom							
Rotational			**Translational**				
R_Z	R_Y	R_X	Z	Y	X		
free	constrained	constrained	constrained	free	free	Bottom surface	
constrained	free	constrained	free	constrained	free	Left and right surface	Rock
constrained	constrained	free	free	free	constrained	Front and back surface	sample node
free	free	free	free	free	free	Top surface	
constrained	constrained	free	constrained	free	constrained	All node	Disc node

3.3. Validation of proposed model in determining forces on disk

Prior to analyzing the disc wear, the accuracy of the numerical method for a given problem must be determined. As already mentioned, there are several methods including the analytical, laboratory, and numerical ones for measuring the force applied to a single disc cutter. The validation of the proposed method is based on the results of Cho et al. [47]. They cut a sample of granite rock using a linear cutting machine and then simulated the process. For the analytical section, the CSM method introduced by Rostami [2] was used. It is noteworthy that the mechanical properties of the specimen were set as in Cho et al. [47], except that the precise cutter geometry CCS was used to model the disc cutter. However, Cho et al. [47] used a V-shaped cutter due to the curvature of the CCS cutter that required a considerable number of small

elements and greatly reduced the computational speed. In Table (3), the absolute mean of the vertical and rolling forces obtained by the proposed method for different penetration depths and cutter distances were compared with other methods. As it can be seen, the results of this method are quite accurate. In the case of a normal force, at a low penetration depth, the result of the analytical method is more than the real data, and with increasing penetration depth, the analytical method estimates a less value. However, the proposed method shows a good agreement with the LCM test. In the case of the rolling force, the analytical method and the method of Cho et al. [47] show greater values at all penetration depths, while the proposed method often estimates relatively smaller values than LCM. According to the numerical modeling, at all penetration depths, with increasing cutter distance, both the normal and shear forces

increase. However, after a certain value (about s/p=15), a significant increase is not observed in the disc cutter forces. This means that the interaction between the side cuts is stopped and each cut acts individually. Such a trend is also visible in the LCM test results.

Figure 5 shows the stresses on the rock sample during cutting with a single cutter disc and a double cutter disc with a penetration depth of 4 mm and a spacing of 40 mm. Figure 6 shows a diagram of normal, rolling, and lateral forces acting on the front and rear cutter discs. It is observed that the

normal and rolling forces applied to the front of disc cutter are slightly higher than the corresponding forces in the rear disc cutter, which is due to the influence of the primary cut on the second cut. The average normal force applied to the front of disc cutter is 219.21 KN, and for the rear disc, it is 162.94 KN. The absolute mean rolling force for the front and rear discs are 15.18 KN and 8.55 KN, respectively, and the mean lateral forces for the front and rear disc are 2.87 KN and -4.64 KN, respectively.

Table 3. Comparison of different methods in predicting the vertical and rolling forces applied to the disc cutter at different penetration depths and different disc cutter distances.

P (mm)	S/P	Mean normal forces (KN)			Mean rolling forces (KN)			
		LCM [47]	Rostami [2]	Presented method	LCM [47]	Rostami [2]	Cho et al. [47]	Presented method
4	5	99.2	137.67	110.76	3.7	13.31	5.3	3.98
	7.5	119.2	141.49	122.4	5.5	13.68	6.3	5.09
	10	122	145.31	130.37	5.8	14.05	7.1	6.22
	12.5	127.7	149.13	135.13	6.3	14.42	7.8	7.73
	15	-	152.95	141.85	-	14.79	8.2	7.82
	20	147.4	160.59	139.76	5.7	15.53	8.1	7.91
6	5	137.2	143.43	142.35	7.5	17.03	12.2	6.43
	7.5	159.1	149.16	160.31	10.7	17.71	13.3	7.63
	10	184.2	154.89	169.58	10.1	18.39	13.7	8.56
	15	172.9	166.35	171.34	10.6	19.75	14.3	10.24
	20	196.7	177.82	180.66	12.9	21.11	14.5	10.71
8	5	167.2	149.19	162.94	13.2	20.50	19.4	8.55
	7.5	212.5	156.83	198.65	17.2	21.55	20.3	10.19
	10	219.3	164.47	205.32	17.3	22.60	21.4	11.41
	12.5	-	172.12	211.77	-	23.65	23.5	13.72
	15	234.6	179.76	217.28	17.6	24.70	24.6	15.06
	20	228.7	195.04	218.08	17.2	26.80	26.2	15.19
10	5	-	154.95	170.33	-	23.86	-	9.89
	7.5	-	164.50	199.64	-	25.33	-	11.21
	10	-	174.06	218.27	-	26.80	-	13.4
	15	-	193.16	227.15	-	29.74	-	18.59
	20	-	212.27	230.89	-	32.68	-	18.62

(a)   **(b)**
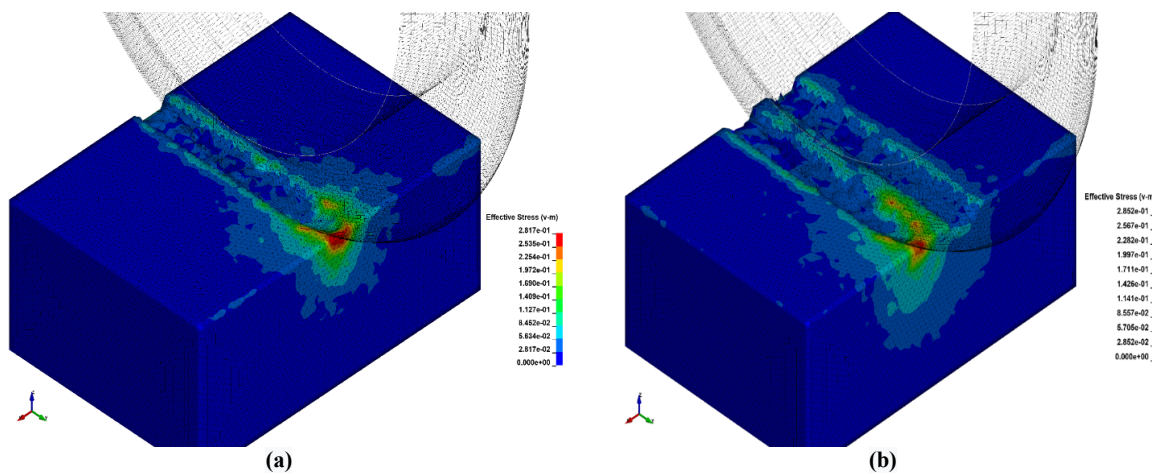
Figure 5. Stresses on a rock sample with a) a single disc cutter; b) a double disc cutter (stress unit GPa).
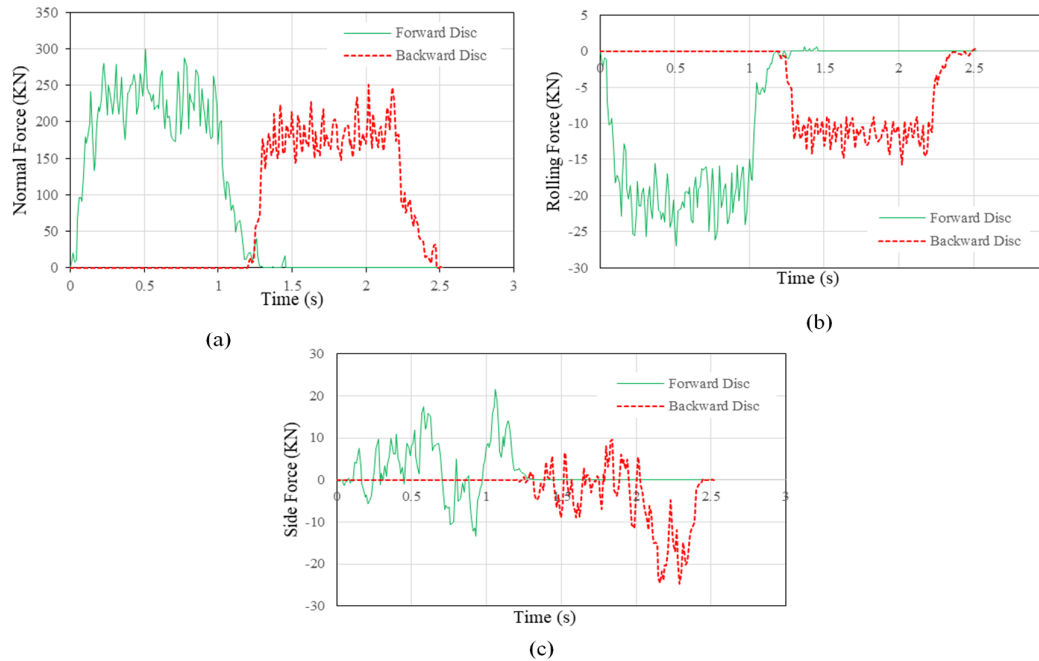
(a)

(b)

(c)

Figure 6. Force diagram applied to the front and rear disc cutters in a binary cut: a) normal force; b) rolling force, c) lateral force.

Figure 7 shows the stress distribution beneath the front and rear discs. In accordance with this figure, it is easy to see the boundary of the crushed zone and the relationship between the side cutting grooves.

3.4. Determining forces applied to worn disc cutter

After validating the numerical method in determining the cutting parameters, the first step in determining the disc cutter wear is to measure the changes in the forces applied to a worn disc. Rostami and Izmir [49] have developed an analytical method for determining the force applied to the disc in hard rocks by considering the

crushing zone pressure beneath the fixed-section disc cutter (ccs). According to their method, the total or consequent force (F_T) applied to the disc cutter is as follows:

$$F_T = \frac{P^0 R T \theta}{\psi + 1} \qquad (10)$$

As P^0 is the base pressure, R is the diameter of the disc cutter, T is the cutter width, and ψ is a constant for the pressure distribution function (usually between -0.2 to -0.2) and decreases with increasing ccs cutter width [50]; the contact angle between the rock and the disc cutter (θ) was also defined previously in Equation (4). In accordance with Equation (10), F_T also increases with cutter wear and increasing cutter tip width.

(a)   (b)
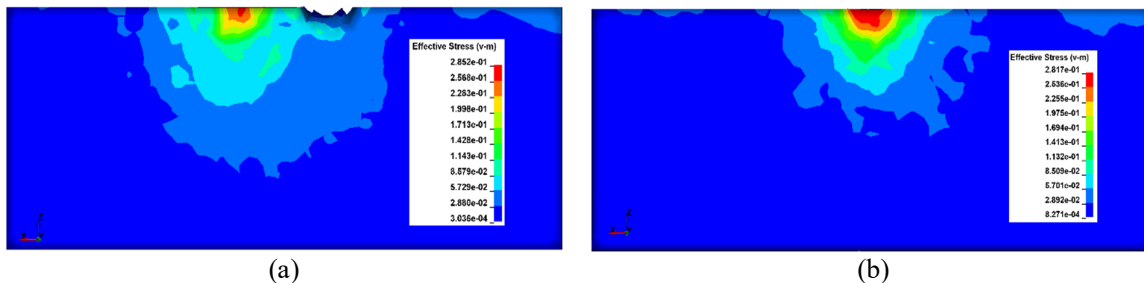
Figure 7. Distribution of stresses in front of disc cutter: a) beneath a single disc cutter; b) beneath rear disc cutter in a double cutter.

The numerical simulations were performed for determining the forces on the worn discs with

varying degrees of abrasion in contact with a rock environment with specifications according to Table

(4). It should be noted that the specifications presented in Table (4) are related to the case study of this research work, which will be discussed in the next section. Initially, the forces applied to the new cutter were simulated with the penetration rates of 4, 6, and 8 mm. In the next step, by assuming a uniform abrasion on the disc cutter, by changing the cutter geometry, an artificial abrasion was created in it and the forces applied on it were again simulated. Figures 8a and 8b show the changes in the normal and rolling forces against ccs type disc cutter wear. Figures 8c and 8d show the average increase in the normal and rolling forces applied to the disc cutter at the mentioned depths. In this form, the normalized force is defined as the ratio of the force applied to the worn cutter to the

force applied to the new cutter. As it could be seen, by increasing the cutter wear to 25 mm, the normal and rolling forces applied to the cutter increased by 2.93 and 2.72 times, respectively. The increase in force is non-linear; as in the first state of wear, it is increased at a relatively low rate and is gradually increased. These forces are increased with a much higher rate for wears greater than 20 mm, which will eventually cause the more wear of cutters that will eventually lead to more wear. Such changes to the increase in the cutter forces due to the changes in the cutter geometry have been addressed in the Bilgin's research work [51]. However, in the Rostami-Izmir equation [49] (Equation 10), the maximum increase in the normal and rotational forces is equal to 2.67.

Table 4. Characteristics of rock for measuring the forces applied to the cutter.

Parameter	Value	Parameter	Value
Density (Kg/m^3)	2.7	Friction angle (degree)	35.2-42.9
Young module (Gpa)	47.3	Uniaxial compressive strength (Mpa)	110
Poisson's ratio	0.2	Tensile strength (Mpa)	7.6
Porosity (%)	0.6-3.2	Hardness on mohs scale	6.5
Quartz (%)	30	Cerchar abrasion index	3.8

(a)

(b)

(c)

(d)
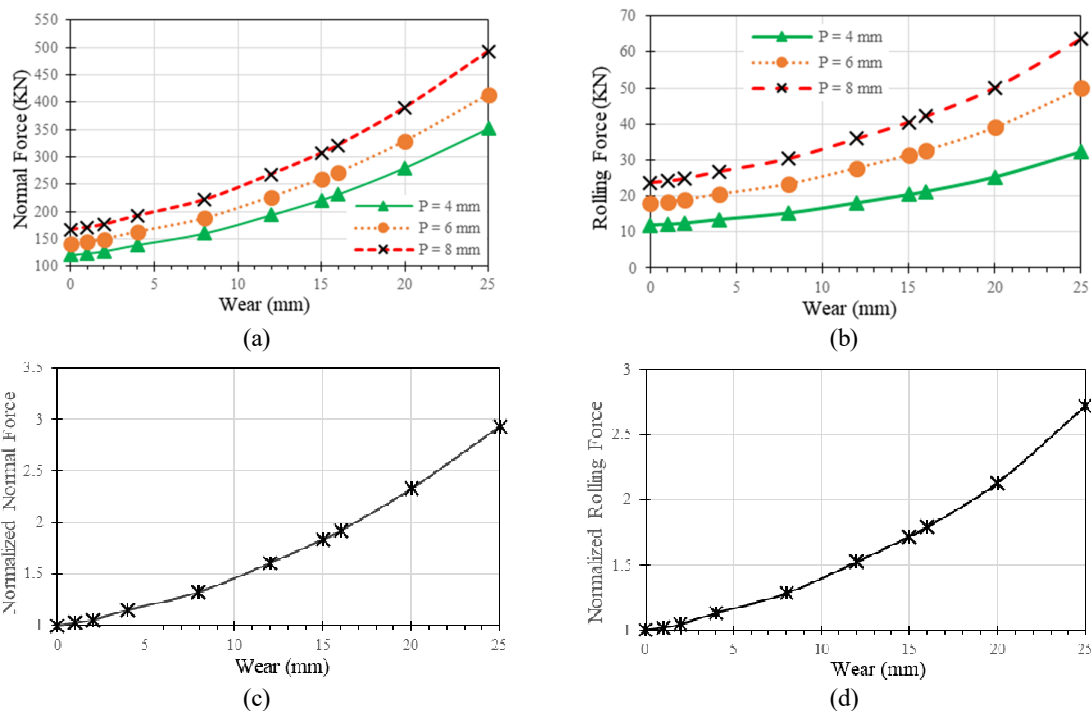
Figure 8. a and b) Normal and rolling force changes on the worn disc cutter at 4, 6, and 8 mm penetration depths; c and d) Average increase coefficients at normal and rolling forces at 4, 6, and 8 mm penetration depths.

4. Disc Cutter wear calculation

In order to calculate the wear of disc cutter using Equation (8), it is necessary to determine the characteristics of the rock environment, the K

coefficient, and the number of discs in the cutter head. The Kani-Sib water transfer tunnel project data was used for the TBM parameters and rock environment characteristics.

4.1. General outline of Kani-sib water transfer tunnel

In order to improve the environmental conditions of the Urmia Lake, a water transfer tunnel was planned in the northwestern Iran. This tunnel carries the Lavin River to the Urmia Lake 35661 m long. The tunnel route is geologically located in the Sanandaj-Sirjan zone. The tunnel route includes the sedimentary, metamorphic, and igneous rocks as well as the alluvial sections. Figure 9 shows the geological profile of the tunnel path. Since the most length of the tunnel was located in hard rock, there was a concern that due to the strength of the rocks, the cutter consumption in this section would increase extremely. Figure 10 shows the types of wear created on the disc cutters associated with this project.
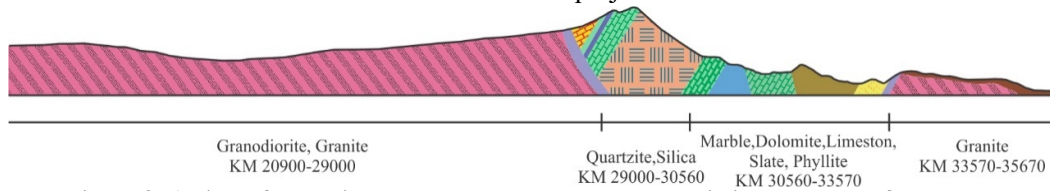

| Granodiorite, Granite KM 20900-29000 | Quartzite,Silica KM 29000-30560 | Marble,Dolomite,Limeston, Slate, Phyllite KM 30560-33570 | Granite KM 33570-35670 |

Figure 9. A view of geological structure zones along the Kani-sib water transfer tunnel.

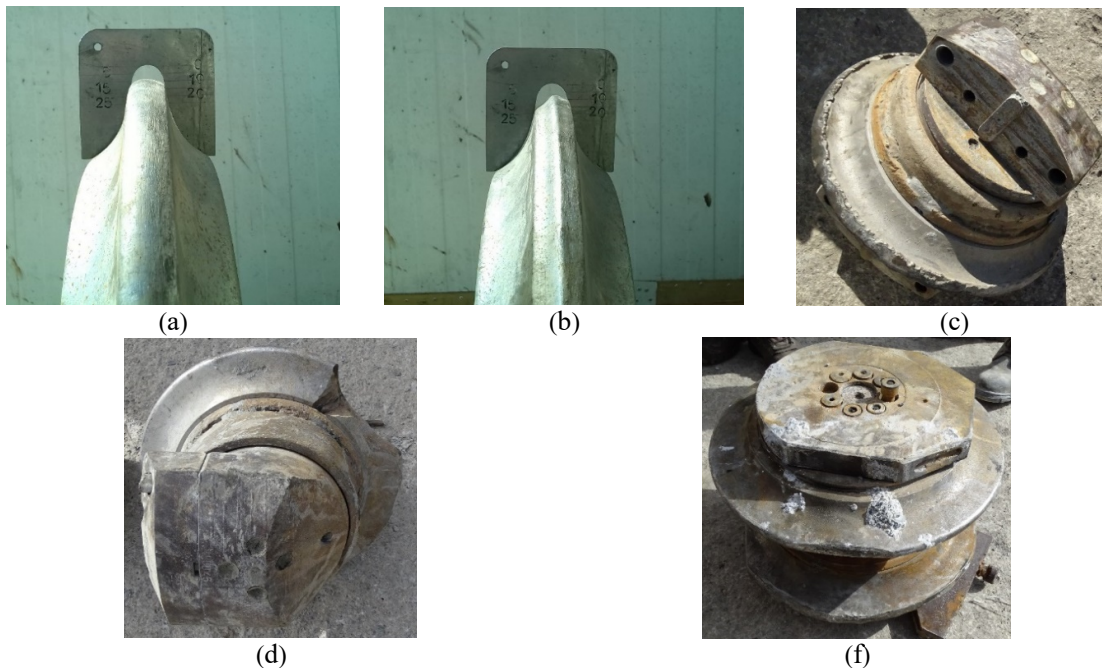(a)   (b)   (c)

(d)   (f)

Figure 10. Types of damage to disc cutter in the Kani-sib water transfer tunnel: (a) uniform normal wear; b) non-uniform normal wear; c) crushing the cutter edge; d) disc cutter ring cracking, f) unilateral flat wear.

4.2. Measurement of *K* coefficient

As stated in the previous section, the K coefficient in Equation (8) depends on the hardness of the disc cutter as it increases with decreasing hardness. In order to increase the life of the cutter in hard rock, the manufacturer hardens the surface with a special heat treatment. Such a treatment gradually reduces the stiffness of the disc from the surface to the core. Therefore, in addition to preventing wear, in the event of a severe impact, the cutters will be deformed to prevent a brittle failure. Instead, the wear resistance at the surface of the cutter is much higher than the interior part. In this work, the hardness of different points on the Wirth disc cutter used in this project was measured using the ASTM standard. Table (5) presents the hardness values of the cutter surface and its core. Given that as the material hardness decreases, its wear resistance decreases, the *K* coefficient is inversely proportional to the hardness of the cutter.

**Table 5. Measured hardness in the surface and core based on the Vickers scale and the ASTM standard.**

Location	Hardness value (HV)			
	Location 1	Location 2	Location 3	Average
Core	421	417	421	420
Surface	848	862	855	855

4.3. Measurement of wear rate in granite zone

The Kani-sib water transfer tunnel was excavated by a mechanized machine. The TBM machine used in this project was manufactured by the NFM Technologies Company with a diameter of 6.32 *m* and a double shield type with 43 cutters mounted on the entire cutter head. The actual shape of TBM, the schematic representation of the whole TBM, and the location of the disks on the cutter head are shown in Figure 11. TBM was equipped with a torque and axial force recording system. In addition, the characteristics of the rock and the data on disc cutter replacement during the project were recorded as a database.

The disc cutter replacement reasons and the consumption number used in the granite zone are presented in Figure 12. As it can be seen in this figure, a variety of factors cause the cutter to be damaged, and these factors change with respect to the position of the disc cutter. For example, in the central disc, often the gripping or jam causes the cutter to be replaced, whereas for the peripheral disc, in addition to gripping, the fracture and crack propagation is the main cause of the cutter replacement. The reasons for disc replacement and their contribution to the final number of disc consumed in the granite zone are presented in Figure 13. According to this figure, normal wear and chipping or mushrooming of disc, two common causes of replacement are about 69% of the replacements. Therefore, by improving the disc condition, their consumption can be significantly reduced.

(a)

(b)

(c)
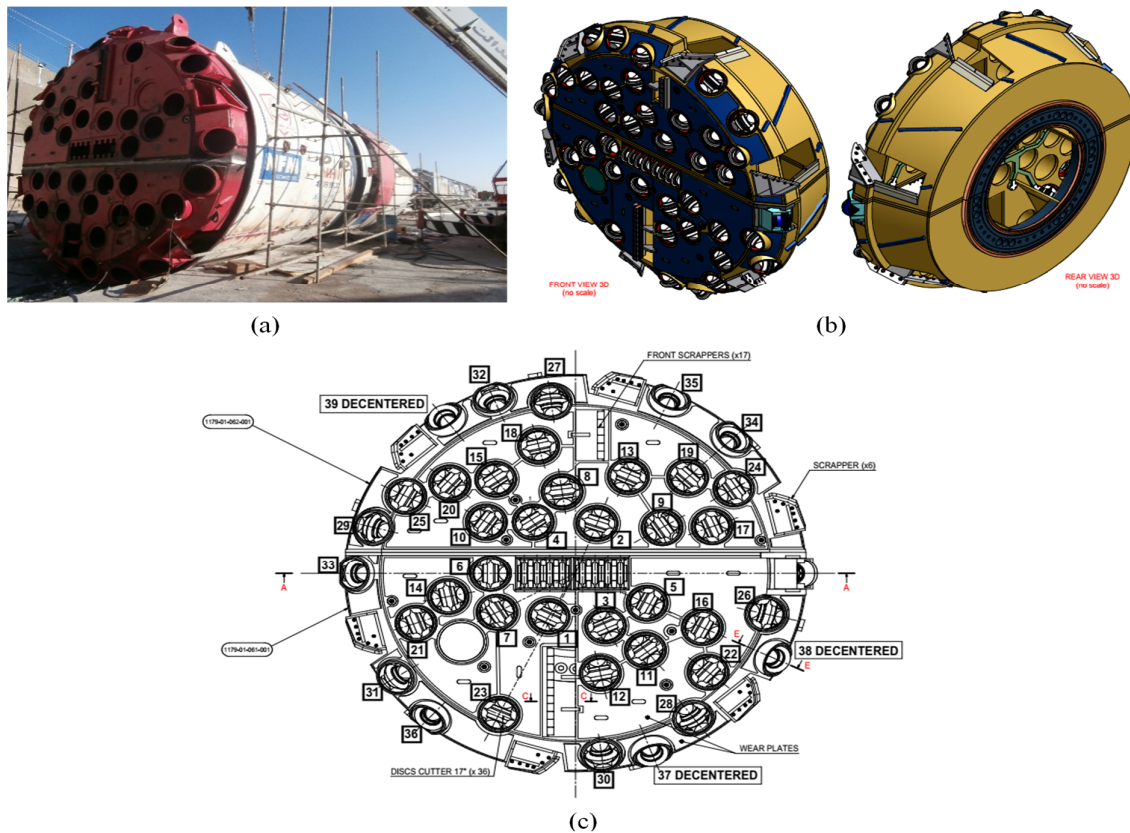
Figure 11. a) Real view; b) 3D schematic view; c) disc cutter location on cutter head.

(a)   (b)
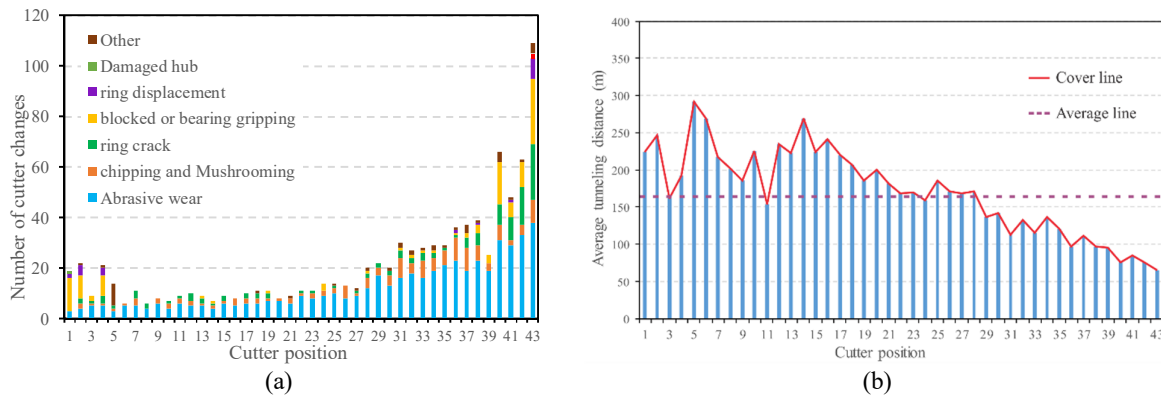
Figure 12. a) Number and causes of disc replacement relative to their position in the granitic zone; b) Average performance of each disc cutter in terms of the tunnel length, taking into account the normal wear on the hard rock zone.

Considering the replaced discs in the hard rock zone due to normal wear and the removal of other discs replaced for other reasons, the performance of all disc (in terms of km of tunnel) was calculated according to their position. This value is called the linear function of disc cutter and is presented in Figure 12b. According to this figure, with the distance from the center of the cutter head, the function of the disc decreased more or less uniformly. In addition, although the number of

central cutter replacements was higher than their adjacent discs in the middle of the cutter head, since only the normal wear was considered for the disc, they showed a relatively good linear performance with the normal wear condition. This result indicates the need to optimize and improve the performance of the central disc against gripping. According to Figure 12b, the average tunneling distance for the entire disc in the granite zone is about 160 m.
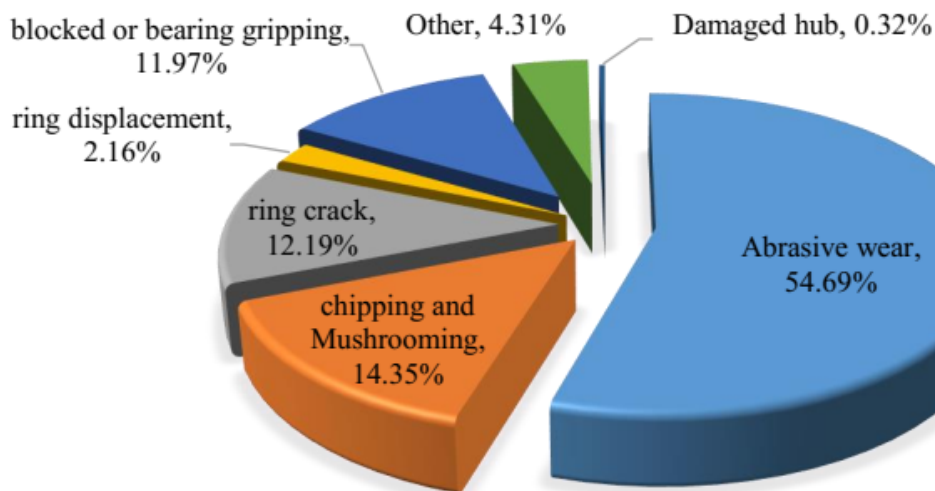
Figure 13. Reasons for replacing disc cutters in the granite zone and their contribution to the total replacement.

The average distance of the disc No. 3 to 7 from the center of cutter head is 1.05 m, and the mean of their function is 196.67 m in one km. This value was chosen in order to compare the results of the numerical model with the experimental results for the disc rotating at a radius of 1.05 m from the center of the cutter head.

In order to model the disc wear, the forces applied to the new disc were calculated. Based on the forces obtained and Equation (8) and the

assumption of a proper advance (L), the volumetric wear of disc cutter (mm^3) was calculated. By having the exact cutter geometry and assuming uniform wear, the volumetric wear is converted to the radial or linear wear. Linear wear is defined as the decrease in the disc radius due to wear, and is expressed in mm. The disc geometry is updated using the obtained wear and applied to the next advance. Then the forces applied to this worn disc are calculated. This process continues until the disc

linear wear reaches a critical level and loses its performance. According to the above description, if the advance length is assumed small enough, the cutter geometry is updated at shorter distances and the wear curve fits more accurately. For such a purpose, distances less than 50 m will give a very good accuracy. On the other hand, the amount of critical wear due to the mechanical properties of the disc, the hardness distribution in the disc, and the manufacturer's recommendation was considered to be equal to 25 mm. The values selected for the wear rate calculation by Equation (8) are listed in Table 6. The variable values (F_n, F_r, L) are also obtained from the numerical modeling results. In addition, the numerical model used for the wear rate calculation is shown in Figure 4.

Table 6. Selected wear rate calculations.

Parameters	Values
Wear rate of energy, I (mm^3/J)	5×10^{-5}
Friction coefficient, μ	0.23
Penetration depth, mm	4, 6, 8
Disc cutter installation radius, m	1.05
Radius of new disc cutter, mm	432

Figure 15 shows the wear values vs. the disc cutter performance installed at a radius of 1.05 m at the penetration depths of 4, 6, and 8 mm in the granite sample. The red line in this diagram is set to the critical value. According to this figure, with increase in the tunneling distance, initially, the disc wear increases gradually with a relative linearly. However, after increasing it to a certain amount, the process is non-linear and significantly increases. Considering the critical amount of wear, the disc cutter life for the penetration depths of 4, 6, and 8 mm is approximately 295, 227, and 200 m, respectively. According to Figure 12, the numerical results for the cutter life were calculated slightly more than the experimental value. The reason for this larger estimate of cutter life is attributable to neglecting the stresses surrounding the rock. The confining stresses changed the rock failure conditions from uniaxial to triaxial and increased the rock failure resistance. A more rock resistance means a shorter disc life.

For this purpose, the main stress fields and their directions were measured in the kani-sib water transfer project. Based on these measurements, the average stresses on each element on the tunnel face are as follow:

$$\sigma_h = 10.12 \, MPa$$

$$\sigma_V = 9.20 \, MPa$$

$$K = \sigma_h/\sigma_V = 1.1$$

Knowing the amount and direction of these stresses, in the next stage of numerical modeling, confining stresses were applied to the rock sample as an initial stress and again, normal and rolling forces applied to the cutter during the rock cutting process were investigated as a function of the wear rate. Figures 14a and 14b show the variations in the forces acting on the cutter with and without the confining stresses. Note that the dotted lines in this figure are the same as those shown in Figures 8a and 8b, and the continuous lines indicate the wear with respect to the confining stresses.

According to these figures, it can be seen that with the initial stresses, the normal forces applied to the cutter are slightly increased, and this increase is intensified with increasing wear rate. On the other hand, in new disks and at a low penetration depth, the variation in the rolling force is negligible. However, at larger depths, the rolling force of the specimen is slightly larger. The routine observed in the normal forces is also observed here so the forces applied to the non-confining and pre-stressed specimens increases with increasing wear.

By evaluating the effect of the confining stresses on the applied forces, as in the previous step, with the aid of Equation (8), the wear rate of the cutter installed at a distance of 1.05 m from the center of the cutter head was calculated in the granite sample by applying the confining stresses. Figure 15 shows the linear wear rate of the disc cutter as a function of the tunneling distance. In this figure, the dotted lines represent the wear values without any initial stress, and the continuous lines are related to the shear process after applying the confining stresses. As it can be seen in Figure 15, the wear rate of the disc cutter is increased such that for a penetration depth of 8 mm and assuming a normal wear, approximately 180 m of tunneling is expected from a standard disc.
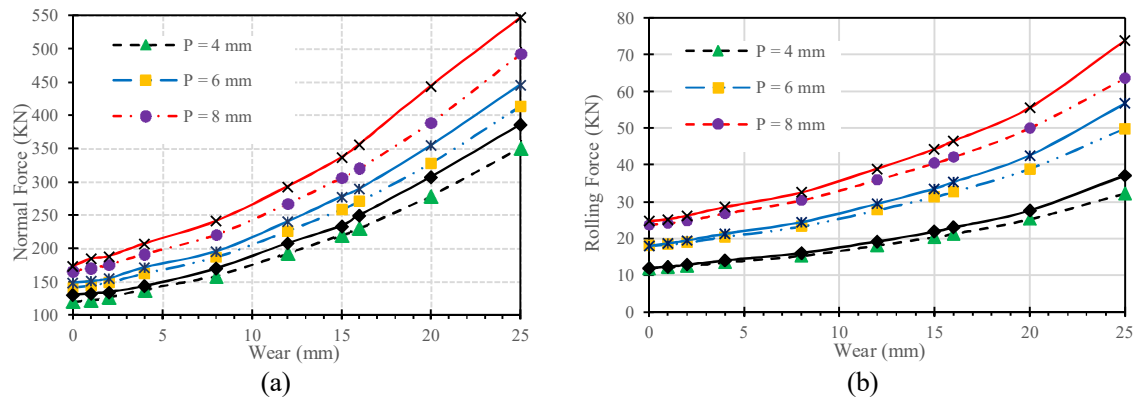
(a)   (b)

Figure 14. Cutter forces with increasing wear: a) normal forces, b) rolling forces for penetrations of 4, 6, and 8 mm.
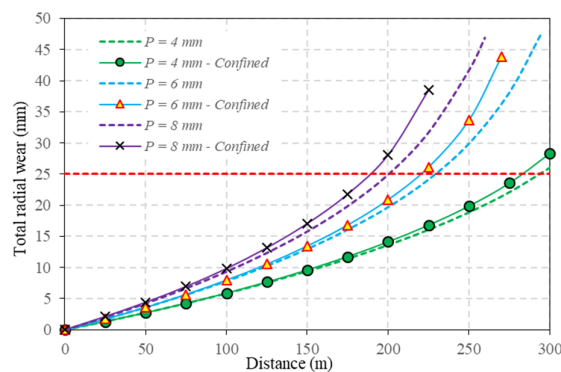

Figure 15. Radial wear of a disc cutter installed at a distance of 1.05 *m* from the center of the cutter head versus the tunneling distance in granite.

As the wear exceeds the critical value, in addition to drastically reducing the efficiency of the disc cutters, the load on them also increases, which may increase the temperature of the disc and increase the probability of the bearing failure or its sealing. A regular inspection and replacement according to a schedule is required to maximize the cutter life, reduce the cutter replacement time, and minimize the costs and scheduling effects.

5. Conclusions

The ability to accurately predict the performance and penetration rate of TBM is one of the main requirements for the accurate project time and cost estimations. However, without considering the wear of disc cutters, this estimation would not be possible. Replacing the disc cutters is a time-consuming and costly action that can dramatically reduce the TBM performance and advancement rates, and has a major impact on the end-time and project cost.

Therefore, in this work, we tried to develop a new approach to estimate disc cutter wear using the 3D numerical modeling of rock and cutter interaction

and compare the results with the other existing methods. For this purpose, a complete database including the rock properties, operating parameters of the machine, and wear rates was created during the excavation of the Kani-Sib water transfer tunnel in the northwestern Iran. The results of this work are as what follows.

- The results obtained show the effectiveness of the proposed method in estimating the forces applied to the new and worn cutters, and also indicate that this method is an effective tool for estimating the disc cutter wear in the diverse operating conditions.
- The forces acting on the disc cutter are a function of its wear rate so that the normal and rolling forces on the cutter increase non-linearly with increasing wear rate, and will be a factor for more wear.
- With increase in the tunneling length, initially, the cutting tool wear increased gradually and relatively linearly. However, after increasing, from a certain value, the process changed to a non-linear form and the wear of cutter increased significantly.

- The causes of disc cutter replacements are different and partially dependent on their location, e.g. for central disc often gripping or jamming, whereas for the peripheral disc, in addition to gripping, the fracture and crack propagation are the common reasons for replacement of the cutters. However, normal wear, crushing, and mushrooming are the major causes of damage to all discs and include 69% of the disc cutter replacements. Therefore, as the disc resistance to these factor improves, its service life will be significantly increased.

- As the wear exceeds the critical value, in addition to drastically reducing the efficiency of the disc cutters, the load on them also increases, which may increase the temperature of the disc and bear and increase the probability of breakdown of the bearing or its sealing. Regular inspections and replacement according to a schedule are required to maximize the cutter life, reduce the cutter replacement time, and minimize the costs and scheduling effects.

For the future research works, it is suggested to:

✓ Consider anisotropy in the rock mechanical properties;
✓ Full-scale simulate the cutter head and tunnel face;
✓ Investigate the effect of discontinuities on the excavation process and the penetration rate.

References

[1]. Bruland, A. (2000). Hard rock tunnel boring, Fakultet for ingeniørvitenskap og teknologi.

[2]. Rostami, J. (1997). Development of a force estimation model for rock fragmentation with disc cutters through theoretical modeling and physical measurement of crushed zone pressure, in, Colorado School of Mines Golden.

[3]. Hassanpour, J., Rostami, J. and Zhao, J. (2011). A new hard rock TBM performance prediction model for project planning, Tunnelling and Underground Space Technology, 26 595-603, doi: https://doi.org/10.1016/j.tust.2011.04.004.

[4]. Maeda, M. and Kushiyama, K. (2005). Use of compact shield tunneling method in urban underground construction, Tunnelling and Underground Space Technology, 20 159-166, doi: https://doi.org/10.1016/j.tust.2003.11.008.

[5]. Roby, J., Sandell, T., Kocab, J. and Lindbergh, L. (2008). The current state of disc cutter design and development directions, in proceeding of 2008 North American Tunneling Conference, SME C, Citeseer, pp. 36-45.

[6]. Tóth, Á., Gong, Q. and Zhao, J. (2013). Case studies of TBM tunneling performance in rock–soil interface mixed ground, Tunnelling and Underground Space Technology, 38 140-150, doi: https://doi.org/10.1016/j.tust.2013.06.001.

[7]. SU, P.c., WANG, W.s., HUO, J.z. and LI, Z. (2010). Optimal Layout Design of Cutters on Tunnel Boring Machine [J], Journal of Northeastern University (Natural Science), 6 877-881.

[8]. Wan, Z., Sha, M. and Zhou, Y. (2002). Study on disc cutters for hard rock (1)-application of TB880E TBM in Qinling tunnel, Modern tunn Technol, 39 1-11, doi: 10.13807/j.cnki.mtt.2002.05.001.

[9]. Schneider, E., Thuro, K. and Galler, R. (2012). Forecasting penetration and wear for TBM drives in hard rock–Results from the ABROCK research project, Geomechanics and Tunnelling, 5 537-546, doi: 10.1002/geot.201200040.

[10]. Plinninger, R.J. (2010). Hardrock abrasivity investigation using the Rock Abrasivity Index (RAI), Williams, *et al*. (Eds.), Geologically Active, Taylor & Francis, London, 34453452.

[11]. Gehring, K. (1995). Prognosis of advance rates and wear for underground mechanized excavations, Felsbau, 13 439-448.

[12]. Hassanpour, J., Rostami, J., Tarigh Azali, S. and Zhao, J. (2014). Introduction of an empirical TBM cutter wear prediction model for pyroclastic and mafic igneous rocks; a case history of Karaj water conveyance tunnel, Iran, Tunnelling and Underground Space Technology, 43 222-231.

[13]. Liu, Q., Liu, J., Pan, Y., Zhang, X., Peng, X., Gong, Q. and Du, L. (2017). A Wear Rule and Cutter Life Prediction Model of a 20-in. TBM Cutter for Granite: A Case Study of a Water Conveyance Tunnel in China, Rock Mechanics and Rock Engineering, 50 1303-1320, doi: 10.1007/s00603-017-1176-4.

[14]. Frenzel, C., Käsling, H. and Thuro, K. (2008). Factors Influencing Disc Cutter Wear, Geomechanics and Tunnelling, 1 55-60, doi: 10.1002/geot.200800006.

[15]. Yang, H., Wang, H. and Zhou, X. (2016). Analysis on the Rock–Cutter Interaction Mechanism During the TBM Tunneling Process, Rock Mechanics and Rock Engineering, 49 1073-1090, doi: 10.1007/s00603-015-0796-9.

[16]. Park, G.I., Jang, S.H., Choe, S.U. and Jeon, S.W. (2006). Prediction of the optimum cutting condition of TBM disc cutter in Korean granite by the linear cutting test, in: Proceedings of the Korean Society for Rock Mechanics conference, Korean Society for Rock Mechanics.

[17]. Gong, Q.M., Jiao, Y.Y. and Zhao, J. (2006). Numerical modelling of the effects of joint spacing on rock fragmentation by TBM cutters, Tunnelling and

Underground Space Technology, 21 46-55, doi: https://doi.org/10.1016/j.tust.2005.06.004.

[18]. Gong, Q.M., Zhao, J. and Hefny, A.M. (2006). Numerical simulation of rock fragmentation process induced by two TBM cutters and cutter spacing optimization, Tunnelling and Underground Space Technology, 21 263, doi: https://doi.org/10.1016/j.tust.2005.12.124.

[19]. Gong, Q.-M., Zhao, J. and Jiao, Y.Y. (2005). Numerical modeling of the effects of joint orientation on rock fragmentation by TBM cutters, Tunnelling and Underground Space Technology, 20 183-191, doi: https://doi.org/10.1016/j.tust.2004.08.006.

[20]. Eftekhari, M., Baghbanan, A. and Bagherpour, R. (2014). The effect of fracture patterns on penetration rate of TBM in fractured rock mass using probabilistic numerical approach, Arabian Journal of Geosciences, 7 5321-5331, doi: 10.1007/s12517-013-1070-7.

[21]. Li, X.F., Li, H.B., Liu, Y.Q., Zhou, Q.C. and Xia, X. (2016). Numerical simulation of rock fragmentation mechanisms subject to wedge penetration for TBMs, Tunnelling and Underground Space Technology, 53 96-108, doi: https://doi.org/10.1016/j.tust.2015.12.010.

[22]. Su, O. and Ali Akcin, N. (2011). Numerical simulation of rock cutting using the discrete element method, International Journal of Rock Mechanics and Mining Sciences, 48 434-442, doi: https://doi.org/10.1016/j.ijrmms.2010.08.012

[23]. Mendoza Rizo, J.A. (2013). Considerations for discrete element modeling of rock cutting, in University of Pittsburgh, Pittsburgh, PA.

[24]. Cho, J.W., Jeon, S., Yu, S.H. and Chang, S.H. (2010). Optimum spacing of TBM disc cutters: A numerical simulation using the 3D dynamic fracturing method, Tunnelling and Underground Space Technology, 25 230-244, doi: https://doi.org/10.1016/j.tust.2009.11.007.

[25]. Menezes, P.L., Lovell, M.R., Avdeev, I.V. and Higgs, C.F. (2014). Studies on the formation of discontinuous rock fragments during cutting operation, International Journal of Rock Mechanics and Mining Sciences, 71 131-142, doi: https://doi.org/10.1016/j.ijrmms.2014.03.019.

[26]. Jaime, M.C., Zhou, Y., Lin, J.S. and Gamwo, I.K. (2015). Finite element modeling of rock cutting and its fragmentation process, International Journal of Rock Mechanics and Mining Sciences, 80 137-146, doi: https://doi.org/10.1016/j.ijrmms.2015.09.004.

[27]. Yu, B. (2005). Numerical simulation of continuous miner rock cutting process, in College of Engineering and Mineral Resources, West Virginia University Libraries, Morgantown, WV.

[28]. Ewendt, D. (1992). Erfassung der Gesteinsabrasivität und Prognose des Werkzeugverschleißes beim maschinellen

Tunnelvortrieb mit Diskenmeißeln, Kurzberichte aus der Bauforschung, 33.

[29]. Wijk, G. (1992). A model of tunnel boring machine performance, Geotechnical & Geological Engineering, 10 19-40, doi: 10.1007/BF00881969.

[30]. Nelson, P., Al-Jalil, Y.A. and Laughton, C. (1994). Tunnel boring machine project data bases and construction simulation, Geotechnical Engineering Center Report GR, 94-94.

[31]. Dahl, F., Grøv, E. and Breivik, T. (2007). Development of a new direct test method for estimating cutter life, based on the Sievers' J miniature drill test, Tunnelling and Underground Space Technology, 22 106-116, doi: https://doi.org/10.1016/j.tust.2006.03.001.

[32]. Maidl, B., Schmid, L., Ritz, W. and Herrenknecht, M. (2008). Hardrock tunnel boring machines, John Wiley & Sons.

[33]. Bieniawski, Z., Celada, B., Galera, J., Tardáguila, I., 2009, Prediction of cutter wear using RME, in: Proc, ITA Congress. Budapest.

[34]. Wang, L., Kang, Y., Cai, Z., Zhang, Q., Zhao, Y., Zhao, H. and Su, P. (2012). The energy method to predict disc cutter wear extent for hard rock TBMs, Tunnelling and Underground Space Technology, 28 183-191, doi: https://doi.org/10.1016/j.tust.2011.11.001.

[35]. Yang, Y., Chen, K., Li, F. and Zhou, J. (2015). Wear prediction model of disc cutter, J China Coal Soc, 40 1290-1296, doi: 10.13225/j.cnki.jccs.2014.3037.

[36]. Macias, F.J. (2016). Hard rock tunnel boring: performance predictions and cutter life assessments.

[37]. Johnson, K.L. (1985). Contact Mechanics, Cambridge University Press, Cambridge.

[38]. Goryacheva, I.G. and Goryachev, A.P. (2006). The wear contact problem with partial slippage, Journal of Applied Mathematics and Mechanics, 70 934-944, doi: https://doi.org/10.1016/j.jappmathmech.2007.01.010.

[39]. Li, F.H., Cai, Z.X. and Kang, Y.L. (2011). A Theoretical Model for Estimating the Wear of the Disc Cutter, Applied Mechanics and Materials, 90-93 2232-2236, doi: 10.4028/www.scientific.net/AMM.90-93.2232.

[40]. Roxborough, F.F. and Phillips, H.R. (1975). Rock excavation by disc cutter, International Journal of Rock Mechanics and Mining Sciences & Geomechanics Abstracts, 12 361-366, doi: https://doi.org/10.1016/0148-9062(75)90547-1.

[41]. Bandini, A., Paolo, B., Bemporad, E., Sebastiani, M. and Chicot, D. (2014). Role of grain boundaries and micro-defects on the mechanical response of a crystalline rock at multiscale, International Journal of Rock Mechanics and Mining Sciences, 71 429-441, doi: https://doi.org/10.1016/j.ijrmms.2014.07.015.

[42]. Massart, T.J. and Selvadurai, A.P.S. (2014). Computational modelling of crack-induced permeability evolution in granite with dilatant cracks, International Journal of Rock Mechanics and Mining Sciences, 70 593-604, doi: https://doi.org/10.1016/j.ijrmms.2014.06.006.

[43]. Simonovski, I. and Cizelj, L. (2011). Computational multiscale modeling of intergranular cracking, Journal of Nuclear Materials, 414 243-250, doi: https://doi.org/ 10.1016/j.jnucmat.2011.03.051.

[44]. Wu, Z. and Wong, L.N.Y. (2012). Frictional crack initiation and propagation analysis using the numerical manifold method, Computers and Geotechnics, 39 38-53, doi: https://doi.org/10.1016/j.compgeo.2011.08.011.

[45]. Efendiev, Y. and Hou, T.Y. (2009). Multiscale finite element methods: theory and applications, Springer Science & Business Media.

[46]. Norouzi, S., Baghbanan, A. and Khani, A. (2013). Investigation of Grain Size Effects on Micro/Macro-Mechanical Properties of Intact Rock Using Voronoi Element—Discrete Element Method Approach, Particulate Science and Technology, 31 507-514, doi: 10.1080/02726351.2013.782929.

[47]. Cho, J.W., Jeon, S., Jeong, H.Y. and Chang, S.H. (2013). Evaluation of cutting efficiency during TBM disc cutter excavation within a Korean granitic rock using linear-cutting-machine testing and photogrammetric measurement, Tunnelling and Underground Space Technology, 35 37-54, doi: https://doi.org/10.1016/ j.tust.2012.08.006.

[48]. Richard, T. (1999). Determination of rock strength from cutting tests, in, University of Minnesota.

[49]. Rostami, J. and Ozdemir, L. (1993). A new model for performance prediction of hard rock TBMs, in: Proceedings of Rapid Excavation and Tunnelling Conference, USA, pp. 794–809.

[50]. Tumac, D. and Balci, C. (2015). Investigations into the cutting characteristics of CCS type disc cutters and the comparison between experimental, theoretical and empirical force estimations, Tunnelling and Underground Space Technology, 45 84-98, doi: https://doi.org/10.1016/ j.tust.2014.09.009.

[51] Bilgin, N., 1977, Investigations into the mechanical cutting characteristics of some medium and high strength rocks, in, University of Newcastle Upon Tyne, UK, pp. 332.

مطالعه عددی تخمین عمر دیسک کاتر ماشین حفر تونل در سنگ‌های سخت

مسعود ظهیری گالشی۱، کامران گشتاسبی۲*، جعفر خادمی۲ و کاوه آهنگری۱

۱- بخش مهندسی معدن، دانشگاه آزاد اسلامی واحد علوم و تحقیقات، تهران، ایران

۲- بخش مهندسی معدن،دانشکده فنی و مهندسی، دانشگاه تربیت مدرس، تهران، ایران

* نویسنده مسئول مکاتبات: goshtasb@modares.ac.ir

چکیده:

بهره‌وری حفاری مکانیزه در سنگ‌های سخت رابطه مستقیمی با کارآیی دیسک کاترها دارد. سایش دیسک کاتر یک عامل مهم تاثیرگذار بر روی عملکرد ماشین حفر تونل (TBM) است. تعویض دیسک کاترها یک اقدام زمان‌بر و هزینه بر است که می‌تواند به طور چشمگیری بهره‌وری TBM و نرخ پیشروی را کاهش دهد و تاثیر عمده‌ای بر زمان نهایی و هزینه پروژه تونلسازی دارد. به خصوص در زمان حفاری در سنگ‌های سخت، تاثیر سایش کاتر در فرآیند حفاری شدیدتر است. به منظور بررسی عملکرد دیسک کاترها ابتدا ضروری است تا فهم عمیقی از مکانیزم برش سنگ داشت و پس از آن شناسایی عوامل اصلی ایجاد کننده سایش اهمیت خواهد داشت. این مطالعه در تلاش است تا یک روش عددی جامع برای تخمین سایش دیسک کاترها معرفی نماید. از اینرو داده‌های میدانی شامل سایش بیش از ۱۰۰۰ قطعه کاتر و پارامترهای زمین‌شناسی در امتداد تونل انتقال آب کانی‌سیب در شمال غربی ایران، در یک پایگاه داده معین جمع‌آوری شده و مورد تحلیل آماری قرار گرفت تا قانون سایش حقیقی کاترها تعیین گردد. نتایج حاصل از روش عددی نشان دهنده آن است که با عبور میزان سایش از ۲۵ میلیمتر، نیروهای نرمال و غلطشی وارد بر دیسک کاتر می‌توانند به ترتیب ۲/۹ و ۲/۷ برابر شوند و با گذر از سایش بحرانی، عملکرد بهینه دیسک‌ها از بین خواهد رفت. این روش همچنین نشان داد که فشارهای محدود کننده وارد بر محیط سنگی باعث افزایش سایش دیسک کاتر خواهد شد. با استفاده از فرمول‌بندی پیشنهادی در این مطالعه، می‌توان نرخ مصرف دیسک کاتر را با دقت بالاتری تخمین زد.

کلمات کلیدی: ماشین حفر تونل، سایش دیسک کاتر، مدل تخمین، نیروی برش، مدل‌سازی عددی.